Article

Experimental Study on Low-Temperature Oxidation Characteristics and Ignition Boundary Conditions of Gasoline/Hydrogenated Catalytic Biodiesel

Sicheng Lai [1], Wenjun Zhong [1], [*], Tamilselvan Pachiannan [2],[3], Zhixia He [1],[2], and Qian Wang [1]

[1] School of Energy Power Engineering, Jiangsu University, Zhenjiang 212013, China
[2] Institute for Energy Research, Jiangsu University, Zhenjiang 212013, China
[3] School of Environment and Safety Engineering, Jiangsu University, Zhenjiang 212013, China
[*] Correspondence: wj_zhong@ujs.edu.cn

Abstract: This study investigates the ignition characteristics of Hydrogenated Catalytic Biodiesel (HCB) with pure gasoline, and diesel. The experiment aims to enhance the ignition characteristics of gasoline fuel by blending it with high-reactivity HCB. It provides experimental data for the fuel blends and offers dependable support for gasoline compression ignition mode applications. To achieve this, the ignition characteristics of various fuels were studied on a variable compression ratio test bench. Experiments were conducted by varying the equivalence ratio and intake temperature of the fuel blends. By analyzing CO emissions and the maximum in-cylinder temperature, we investigated the low-temperature oxidation characteristics of the fuels. Simultaneously, we identified the critical compression ratio and critical temperature as indicators of the ignition boundaries. Finally, this study examined the heat release behavior of the fuels at low temperatures and discussed their combustion characteristics under high-temperature conditions through the heat release rate analysis. The study indicates that with the increase of HCB in the blend, the low-temperature oxidation characteristics are significantly enhanced. However, the ignition boundaries are lowered, and more pronounced secondary heat release combustion behavior is observed. When the blending ratio reaches 50% namely G50H50, it exhibits low-temperature oxidation characteristics and a secondary heat release rate similar to diesel. Their critical compression ratios are 6.8 and 6.5, and the critical temperatures are 838.74 K and 881.41 K respectively. Hence the G50H50 blend holds the potential to serve as a substitute for diesel fuel in compression ignition engines. The increase in intake temperature and equivalence ratio can also enhance low-temperature oxidation characteristics and lower the ignition boundaries. Simultaneously, they exert a certain influence on the peak and phase of the heat release rate.

Keywords: gasoline compression ignition; gasoline; hydrogenated catalyzed biodiesel; low-temperature oxidation characteristics; variable compression ratio

1. Introduction

The National Bureau of Statistics on Vehicle Ownership in China reported that in 2022 civilian passenger vehicle ownership in China had reached 277 million, up 6.1%, and car ownership had reached 311 million, up 5.7% than in 2021 [1]. In light of the significant levels of combustion emissions produced by several internal combustion engines, it is crucial to prioritize research efforts aimed at enhancing energy efficiency and reducing emissions across various engine categories. The significance of this research lies in its potential to mitigate carbon emissions, safeguard the environment, and promote human well-being.

In recent years, to break through the perception of existing combustion methods and to change the process of combustion reaction, some studies have proposed new models of low-temperature combustion, and

the existing new combustion modes are Homogeneous Charge Compression Ignition (HCCI) [2,3], Premixed Charge Compression Ignition (PCCI) [4], Reactivity Controlled Compression Ignition (RCCI) [5, 6], and Gasoline Compression Ignition (GCI) [7, 8], etc. Among them, gasoline compression ignition is considered one of the most potential new combustion modes to improve thermal efficiency and reduce emissions.

Johansson et al. [9] from Lund University, Sweden first introduced the concept of direct compression ignition of high-octane gasoline in a heavy-duty diesel engine, known as gasoline partially premixed combustion (PPC), also known as gasoline compression ignition, in 2005. Hildingsson et al. [10] studied the emission characteristics of gasoline compression ignition mode at different loads for gasoline and diesel with different octane values. It has been observed that the utilization of high-octane gasoline offers advantages in terms of internal combustion engine emissions at low loads, while the preference shifts to low-octane gasoline for optimizing internal combustion engine combustion at high loads. Unlike other LTC combustion modes, it is not limited by the ignition method or complex fuel injection system and has a wide range of fuel combustion conditions and clean combustion capability [11 – 16]. However, GCI still has many limitations that need to be solved, for example, when gasoline is used as a fuel, good combustion performance and low pollutant emissions can be obtained due to the high volatility of gasoline, which is easy to mix well with air. However, the high-octane number and high ignition temperature of gasoline make it difficult to ignite and burn stably at low loads, while at high loads it causes excessive pressure rise rate and poor soot emissions and so on [17]. The high cetane number and high viscosity diesel fuel can be blended with gasoline to obtain a lower octane number and excellent ignition performance. Kalghatgi GT et al. [18, 19] conducted an experimental study on the combustion and emission characteristics of gasoline/diesel blends with different blends in a light-duty common rail diesel engine. The result shows that gasoline/diesel blend fuel can reduce soot emissions compared to pure diesel, and can keep the NOx at a lower level while maintaining higher combustion efficiency under all operating conditions.

Biodiesel exhibits significant potential as a sustainable energy alternative. When comparing biodiesel to petroleum-based diesel, it is seen that biodiesel exhibits a greater cetane number and oxygen concentration, hence facilitating improved ignition and complete combustion. The current study on GCI combustion is mostly focused on the utilization of biodiesel as a substitute for petroleum-based diesel in the blending of gasoline, which represents a novel fuel-blending approach. Adams [20] et al. studied the combustion and emission characteristics of GCI engines by adding 5% and 10% biodiesel to gasoline and found that: these blends require lower intake gas temperature compared to pure gasoline and increased the combustion stability. By blending biodiesel with gasoline, it is possible to improve the difficulty in the ignition, stable combustion, and high-pressure rise rate. This indicates that research primarily focuses on biodiesel fuel, particularly first-generation biodiesel, with fast compressors or shock tubes. However, there is limited information available regarding the self-ignition properties of second-generation hydrogenation-catalyzed biodiesel. Our research group performed a comprehensive investigation on rapid compression [21]. The initial assessment of the fast compressor test serves as an introductory step in investigating the phenomena of fuel self-ignition and reaction kinetics. However, it is important to note that this test alone does not provide a comprehensive solution to address the challenges associated with low-load ignition in gasoline/HCB blended fuel utilized in GCI combustion mode. The self-ignition of fuel is significantly influenced by the characteristics of its low-temperature oxidation. Excessive low-temperature oxidation activity in gasoline engines can lead to engine detonation, whereas in diesel engines, a certain level of fuel oxidation activity is necessary to facilitate auto-ignition of the fuel at the top dead center [22]. Furthermore, the ignition delay time of fuel is significantly influenced by its low-temperature oxidation activity, which greatly affects the cold starting capability and thermal efficiency of the compression ignition engine [23].

To effectively address the challenges of low-load ignition in GCI mode, there is an urgent need to comprehend the role of gasoline's low-temperature oxidation characteristics in fuel compression combustion, as well as the impact of blending high-reactivity fuel HCB on fuel compression combustion characteristics. Therefore, this study conducted experiments on a variable compression ratio test bench, by varying the blending ratio, equivalence ratio, and intake temperature of the blended fuel. To gain a better understanding of the compression combustion characteristics of the blended fuel during the compression process, we analyzed the variations in CO emissions and maximum in-cylinder temperature by changing the compression ratio. Additionally, we defined critical compression ratios and critical temperatures to find out the ignition

boundaries. Simultaneously, this study integrates heat release rate results to examine low-temperature oxidation heat release and high-temperature combustion behavior. The objective of these experimental analyses is to get an in-depth understanding of the combustion characteristics shown by gasoline when combined with HCB. Furthermore, our objective is to offer significant assistance in tackling the difficulties associated with low-load ignition in gasoline combustion.

2. Experimental Principles and Procedures

2.1. Experimental Principles

In this study, the low-temperature oxidation characteristics of the fuel are studied in a modified variable compression ratio test bench, which is used to test the oxidation activity of the fuel before and after self-ignition. The variable compression ratio test bench is closer to the actual combustion process of an internal combustion engine than other self-ignition research devices such as shock tubes or rapid compressors. The process of adjusting the compression ratio of the engine can be realized by analyzing the compression and ignition process of the fuel in detail and obtaining the data of CO, CO_2, pressure, and heat release rate of the fuel at different stages from low-temperature oxidation to ignition, from which the degree of oxidation at each stage can be assessed and analyzed so that the low-temperature oxidation activity of the fuel can be studied.

The experimental schematic of a variable compression ratio test bench is shown in Figure 1 and this device has been widely used for oxidation ignition studies of various fuels [24,25]. The test bench is mainly composed of a variable compression ratio engine, cooling water system, air intake system, fuel supply system, data acquisition system, etc.
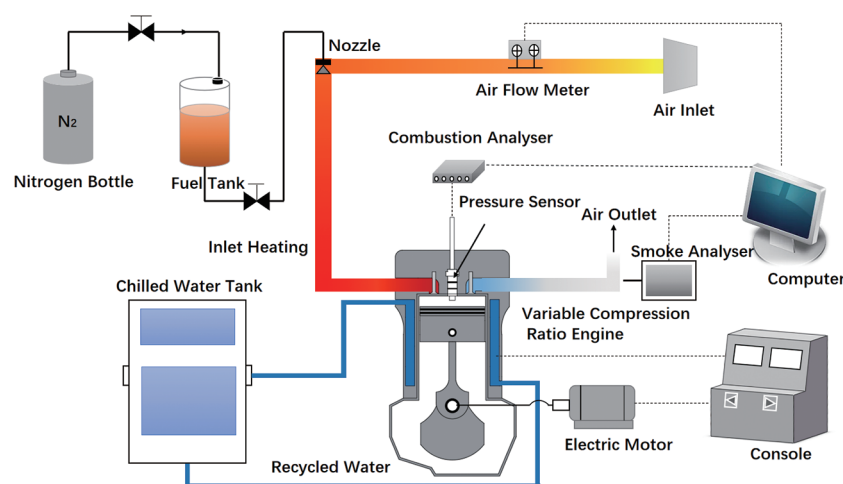

Figure 1. Experimental schematic of a variable compression ratio test bench.

The variable compression ratio engine has an adjustable compression ratio from 4–15, with an accuracy of 0.1. The engine is driven by an electric motor and the rotational speed can be adjusted to maintain a stable level of either 600 rpm or 900 rpm, and temperature of the engine cylinder wall jacket is controlled by circulating cooling water. The air intake system with an airflow meter installed at the intake port monitors the intake volume, and the entire intake piping is arranged with heating and insulation devices to regulate the premixed intake air temperature up to 513 K. The fuel injection system uses high-pressure nitrogen-driven injection, and the nitrogen pressure can be controlled from 2 to 10 MPa. The delivery pipe between the fuel tank and the nozzle is wrapped with a heating band to ensure that the initial temperature of the fuel remains constant and unaffected by the transportation process. The gasoline direct injection electric control nozzle installed vertically above the air intake pipe, with adjustable nozzle injection frequency and injection pulse width. To reach the desired fuel flow during the specified equivalent ratio, it is necessary to adjust the injection frequency and pulse width before each experiment. Additionally, it is important to ensure that the distance between the nozzle and the engine is adequate to provide effective premixing of fuel and air. Engine,

nozzle, intake air, and other related parameters are adjusted by the control unit. The exhaust duct is provided with sampling holes to connect to the flue gas analyzer, and a multi-stage filtering device is provided in front of the flue gas analyzer to cool the flue gas with water and organic solvents to filter the unburned hydrocarbons in the flue gas and prevent them from clogging the flue gas analyzer. The engine body is equipped with a pressure sensor connected to a combustion analyzer to monitor cylinder pressure, and both the combustion analyzer and the flue gas analyzer are connected to a computer to ensure real-time measurements. More detailed parameters of this variable compression ratio test stand can be found in the previous studies [26,27].

2.2. Chemical and Physical Characteristics of Fuel

In this study, gasoline was blended with HCB to study the low-temperature oxidation characteristics of the fuel mixture by varying the compression ratio, blending ratio, equivalence ratio, and inlet gas temperature. The GC-MS (Gas Chromatography and Mass Spectrometry) test results of HCB and its main components are shown in Figure 2.
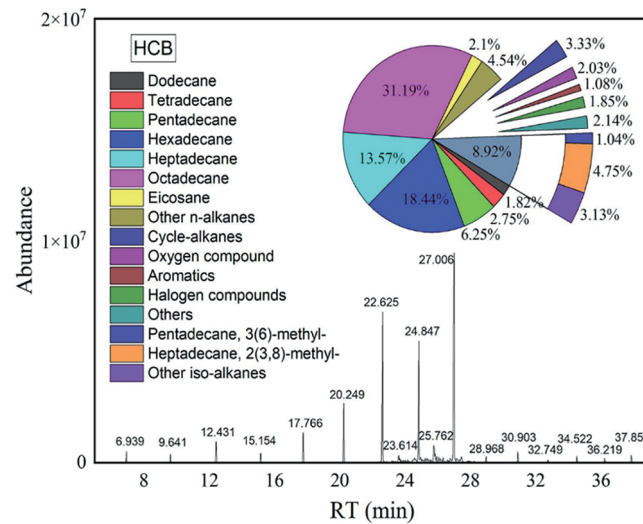
Figure 2. GC-MS result of hydrogenated catalytic biodiesel.

The main properties of the different types of fuels are listed in Table 1. This research also investigates four different blending ratio of blended fuels, which include as G90H10, G80H20, G70H30, G50H50. Some of the chemical and physical properties of the blended fuel can also be calculated according to the relevant formulas. The specific formulas are shown in Equations (1)–(5).

Table 1. Properties of different fuel used in the current experiment.

Fuels Properties	Gasoline	Diesel	HCB	G90H10	G80H20	G70H30	G50H50
Density (20 °C) kg/m³	762	830	791	764.9	767.8	770.7	776.5
Cetane number	14	51	84	21	28	35	49
Viscosity (40 °C) mm²/s	0.62	2.5	3.3	0.7328	0.8662	1.0238	1.4304
Oxygen content (m/m)	<2.7	0	0	<2.43	<2.16	<1.89	<1.4
Low heating value (MJ/kg)	42.7	40.2	44.0	42.83	42.98	43.10	43.36

$$\ln \eta = \sum_{i=1}^{2} \left(\chi_i \ln \eta_i \right) \qquad (1)$$

η represents the viscosity of the blended fuel, η_i represents the viscosity of each fuel, χ_i represents the proportion of each fuel.

$$\rho = \sum_{i=1}^{2} \left(\chi_i \rho_i \right) \qquad (2)$$

ρ represents the density of the blended fuel, ρ_i represents the density of each fuel, χ_i represents the

proportion of each fuel.

$$Hu = \sum_{i=1}^{2} (\chi_i \rho_i Hu_i) / \sum_{i=1}^{2} (\chi_i \rho_i) \tag{3}$$

Hu represents the low heating value of the blended fuel, Hu_i represents the low heating value of each fuel, ρ_i represents the density of each fuel, χ_i represents the proportion of each fuel.

$$CN = \sum_{i=1}^{2} (\chi_i CN_i) \tag{4}$$

CN represents the density of the blended fuel, CN_i represents the density of each fuel, χ_i represents the proportion of each fuel.

$$O = \sum_{i=1}^{2} (\chi_i O_i) \tag{5}$$

O represents the oxygen content of the blended fuel, O_i represents the oxygen content of each fuel, χ_i represents the proportion of each fuel.

2.3. Low-Temperature Oxidation Characteristics of Fuel

During the low-temperature oxidation, a significant amount of carbon monoxide (CO) is generated from the fuel. CO is primarily formed in the regions of the combustion chamber where the low-temperature reactions are active. Its primary origin can be associated with the aldehyde's hydrogen extraction reaction that occurs during the process of low-temperature oxidation [28]. At lower temperatures, CO is difficult to oxidize further into CO_2 [29, 30]. However, in high-temperature environments, CO undergoes further oxidation. Therefore, only significant amounts of CO are detected during low-temperature oxidation processes. The exothermic phenomenon is inevitably accompanied by the low-temperature oxidation process, and the comparison of the maximum cylinder temperature can reflect the strength of the low-temperature oxidation characteristics. Therefore, in the variable compression ratio test bench, the CO emissions and the maximum cylinder temperature can be used to assess the low-temperature oxidation characteristics of the fuel after the compression process inside the cylinder. Figure 3 illustrates the variation of CO emissions and the maximum in-cylinder temperature of the G90H10 fuel during compression ratios. With the increase in compression ratio, the fuel blends undergo four stages: NO-load, Low-Temperature Oxidation (LTO), Negative Temperature Coefficient (NTC), and High-Temperature Combustion (HTC) [31].
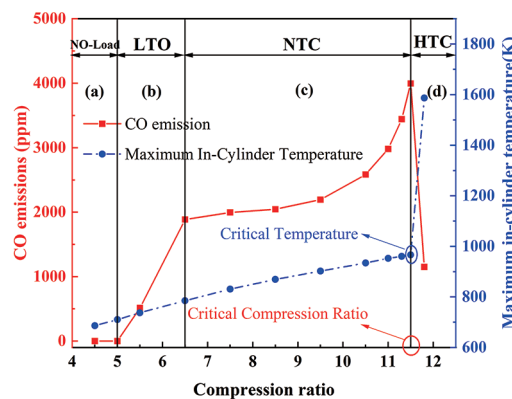

Figure 3. CO emission and maximum in-cylinder temperature of G90H10 with change in compression ratio.

During the low compression ratio (referred to as region a), the absence of carbon monoxide (CO) in the exhaust gases indicates that the fuel is in a state of NO-load stage. As the compression ratio increases, the emission of CO begins to appear and increases rapidly, indicating the onset of the LTO stage (region b). Subsequently, it enters the NTC region (region c), where the in-cylinder temperature suppresses the low-temperature reaction pathways of the fuel [32]. As the compression ratio increases further, the CO emissions exhibit a gradually increasing growth rate. Finally, it enters the HTC stage, and the carbon monoxide (CO) emissions reach their maximum level and subsequently experience a rapid decline. This indicates complete compression combustion of the fuel (region d). The Critical Compression Ratio (CCR) refers to the

compression ratio at which the CO emissions reach the maximum value, which is indicated by the red circle in the figure. The CCR corresponds to the oxidation and combustion stages of the fuel before and after it, respectively. Therefore, by comparing the magnitudes of CCR, it can reflect the ignition boundaries of different fuels. As the compression ratio is increased there is a corresponding gradual rise in the maximum temperature within the combustion chamber. When the ignition process takes place inside the cylinder, there is a significant and rapid rise in the maximum temperature within the cylinder. The critical temperature, denoted by the blue circle, is the upper limit of the in-cylinder temperature before ignition.

In this study, the least square method is employed to perform linear fitting on the CO emissions and maximum in-cylinder temperature within the LTO and NTC regions. The assessment of the strength of the low-temperature oxidation properties can be performed by analyzing the slope of the linear fit lines. This analytical approach helps us understand the variations in CO emissions and maximum in-cylinder temperature during low-temperature oxidation processes under different operating conditions. It also aids in determining the level of low-temperature oxidation activity. The principle and equation of the least square method are as follows:

Calculate the mean of the measured object and the measured value:

$$\bar{x} = (x_1 + x_2 + ... + x_n)/n \tag{6}$$

$$\bar{y} = (y_1 + y_2 + ... + y_n)/n \tag{7}$$

Calculate the slope of the fitted curve, K:

$$K = \sum \left[(x_i - \bar{x})*(y_i - \bar{y}))/\sum((x_i - \bar{x})^2 \right] \tag{8}$$

Calculate the intercept of the fitted curve, b:

$$b = \bar{y} - K*\bar{x} \tag{9}$$

Calculate the standard error of the measured object, SE:

$$SE = \sqrt{MSE/n} \tag{10}$$

$$MSE = \sum \left(y_i - \hat{y}_i \right)^2 /n \tag{11}$$

where x_i is the i_{th} measured object, y_i is the i_{th} measured value, n is the number of measured objects, and $\hat{y}$ is the predicted measured value corresponding to the fitted curve.

2.4. Experimental Procedure

In this test, the engine speed is fixed at 600 rpm and the circulating cooling water is fixed at 90 ℃. Considering the high freezing point of HCB, the temperature of the heating band on the oil tank and the oil delivery pipe was set to 30 ℃. Considering the high distillation temperature of the fuel, the inlet air temperature is set to the maximum safe temperature of 513 K for the equipment. Due to equipment limitations, the experimental setup needs to maintain CCR of all fuels within a reasonable range. Therefore, the equivalence ratios are set at 0.10, 0.15, and 0.20, with a primary focus on the 0.10 condition. All the fuels are tested from the initial compression ratio of 4.5 to the compression ratio at which the fuel is burned and then the increase of compression ratio is stopped (when the critical compression ratio is reached), as shown in Table 2.

Table 2. Test scheme of cryogenic oxidation and compression ignition experiment.

Fuel	Gasoline Blending Ratio	Equivalent Ratio	Inlet Temperature /K
Gasoline	100 (G100)	0.10	513
	90 (G90H10)	0.10	513
Gasoline /HCB	80 (G80H20)	0.10, 0.15, 0.20	513
	70 (G70H30)	0.10	513
	50 (G50H50)	0.10	433, 473, 513
Diesel	0	0.10	433, 473, 513

3. Results and Discussion

3.1. Effect of Blend Ratio on the Low-Temperature Oxidation Characteristics

The blending of high-reactive HCB fuel will inevitably enhance the low-temperature oxidation activity of the fuel blends. Therefore, an initial investigation was conducted to examine the impact of different proportions of HCB on the fuel blends. These results were compared with diesel and gasoline to gain a deeper understanding of the compression ignition characteristics.

Figure 4 shows the results of CO emissions and maximum in-cylinder temperature for different fuels at different compression ratios, during the intake temperature of 513 K and an equivalence ratio of 0.1. Simultaneously, the bar charts show the changes in the respective magnitudes of growth.
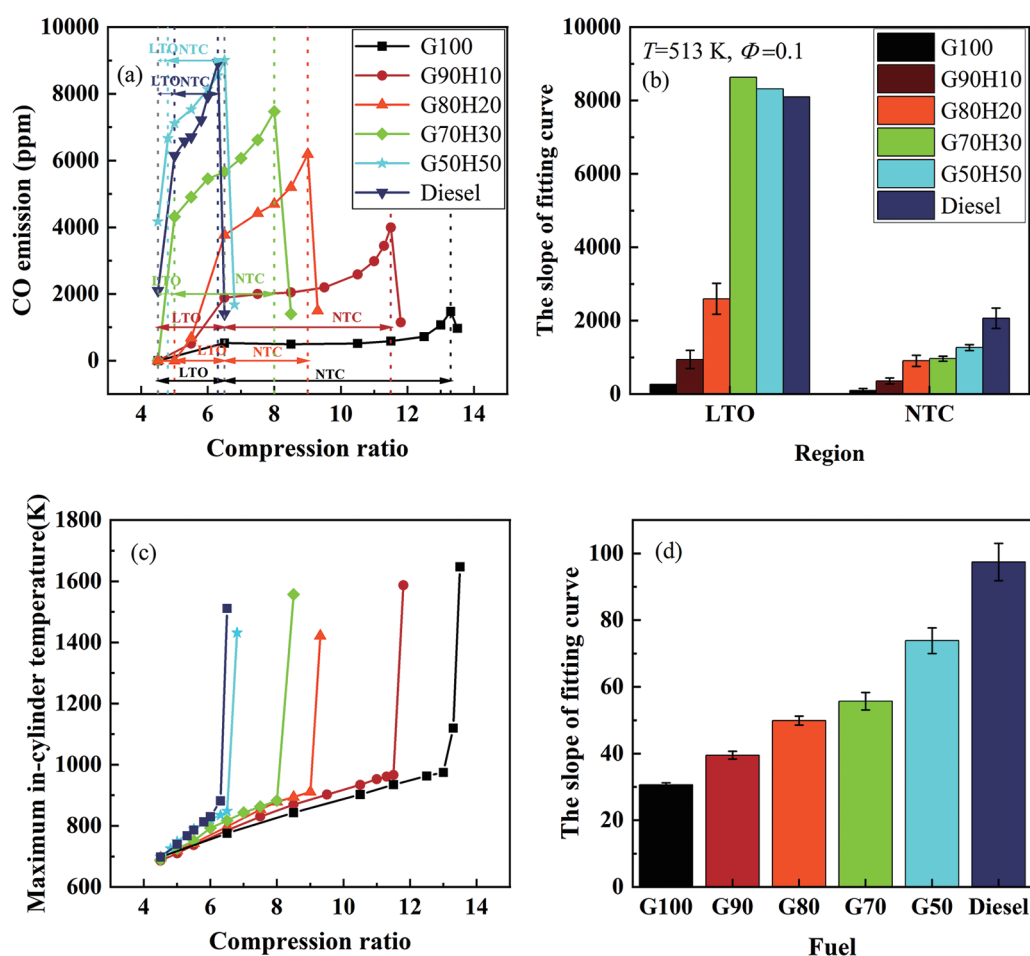
Figure 4. (**a**) CO Emissions, (**b**) CO Emissions Fit Curve Slope, (**c**) Maximum In-Cylinder Temperature, (**d**) Maximum In-Cylinder Temperature Fit Curve Slope of different fuels.

Figure 4a demonstrates that the fuel blends with varying blend ratios show noticeable variations in carbon monoxide (CO) emissions during the low-temperature oxidation phase. It has been observed that the peak CO emission for pure gasoline G100 is approximately 1000 ppm, whereas, for G50H50, the peak CO emission level can significantly increase, reaching up to approximately 9000 ppm. Further, as the blending ratio increases, there is a notable increase in the peak level of CO emissions. This implies that with an increase in the amount of HCB in the blend, there is a corresponding notable increase in the CO emissions, at the same compression ratio.

Furthermore, from Figure 4b, it can be observed that in the LTO region, there is a significant increase in the volume of CO emissions as the blending ratio rises from 20% to 30%. However, subsequent increases in the blending ratio have a negligible effect on the rate of increase. In the NTC region, the rise in CO emissions

is notably lower for low HCB blends than the higher HCB blends. Furthermore, as the blending ratio increases, the magnitude of CO emission escalation exhibits a near-linear trend of gradual augmentation, and the NTC trend in CO emissions becomes progressively weaker. The primary reason for this phenomenon can be attributed to the composition of HCB, which predominantly comprises high-reactivity long straight-chain alkanes with high reactivity. At low temperatures, the reactivity of low-temperature reactions is primarily governed by the initial oxidation of alkyl radicals: $R + O_2 \rightarrow \cdot RO_2$, as well as the isomerization reaction of alkyl peroxy radicals: $RO_2 \rightarrow \cdot QOOH$ [33,34]. These reactions are also the reasons for the occurrence of the low-temperature oxidation stage and are key factors in the ignition process. Therefore, blending HCB can compensate the low oxidation activity of gasoline. With the increasing proportion of HCB in the blend, the low-temperature chain branching reactions in the low-temperature oxidation process occur at a faster rate, leading to enhanced low-temperature oxidation activity of the blended fuel and higher CO emissions. Within the LTO and NTC regions, the increase in CO emissions is more pronounced. Especially when the blending ratio is 50%, the CO emissions and the magnitude of increase for the blended fuel G50H50 closely resemble those of diesel, exhibiting a high degree of alignment.

It can be observed from Figure 4c that, as the blending ratio increases the magnitude of rise in maximum in-cylinder temperature during the low-temperature oxidation process also increases. This is due to the intensified low-temperature oxidation activity, resulting in the release of more heat and consequently raising the in-cylinder temperature. It is important to acknowledge that the lower reactivity of G100 requires a higher compression ratio to achieve compression ignition. For this case, the extremely high compression ratio results in the maximum in-cylinder temperature reaching the temperature required for CO oxidation leading to a secondary rise.

During the low-temperature oxidation process, Figure 4d shows that the magnitude of the rise in maximum in-cylinder temperature follows a linear increasing pattern with an increase in blending ratio. It indicates that increasing the blending ratio of HCB can significantly enhance the low-temperature oxidation characteristics of the blended fuel. The G50H50 blend exhibits a close resemblance to diesel in terms of low-temperature oxidation characteristics, with a slightly lower magnitude of increasing maximum in-cylinder temperature compared to diesel. Therefore, increasing the blending ratio of HCB contributes to enhancing the low-temperature oxidation characteristics and brings the blended fuel performance level closer to that of diesel.

Figure 5 shows the ignition boundaries of gasoline/HCB fuel blends at various blending ratios. From Figure 5a, it can be observed that the CCR for G100 is 13.5, whereas after blending with 10% HCB, the CCR decreases to 11.8. Subsequently, as the proportion of HCB increased further, CCR decreased again and to a greater extent, reaching 9.3. With further increase in the proportion of HCB, the rate of reduction in CCR noticeably slowed down, reaching 8.5 for G70H30 and 6.8 for G50H50. Therefore, when the blending ratio is below 20%, the CCR decreases rapidly, whereas when the blending ratio surpasses 20%, the rate of reduction slows down. It is worth noting that the CCR of G50H50 is very close to the CCR of diesel, which is 6.5.

It can be observed from Figure 5b that the addition of HCB in the blend, decreases the critical temperature sharply. Furthermore, as the blending ratio increases, the critical temperature continues to decrease, and the rate of decrease slows down. This suggests that the addition of high-reactivity fuel and the reduction in critical temperature are not in a linear relationship. Simultaneously, it can also be observed from the figure that the critical temperature of G70H30 is very close to that of diesel, while the critical temperature of G50H50 is slightly lower than that of diesel. It is concluded that the ignition boundary of G50H50 is very close to that of diesel fuel.
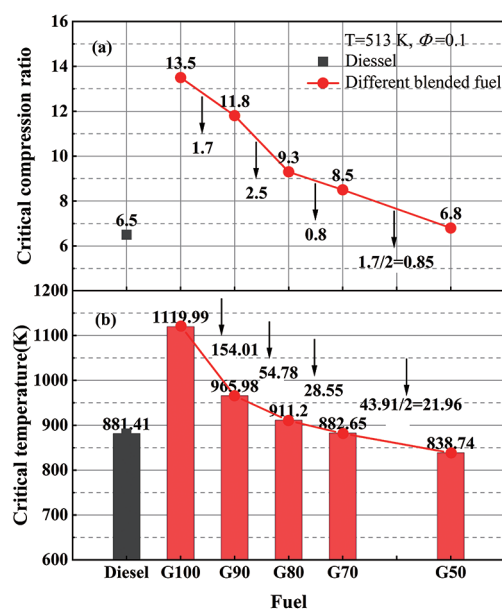
Figure 5. (**a**) Critical Compression Ratio and (**b**) Critical Temperature of different fuels.

Figure 6 shows the heat release rates of different fuel blends at compression ratios of 4.5, 6.5, and CCR. In correspondence with Figure 4a, it can be observed that both G50H50 and diesel fuels exhibited carbon monoxide (CO) emissions at a compression ratio of 4.5. While the remaining fuels failed to produce any CO production. Therefore, it can be observed from Figure 6a that G50H50 exhibits higher CO emissions and higher peak heat release rates compared to diesel. However, other fuels have heat release rate curves that can be associated with the NO-load curve, as they do not produce CO.
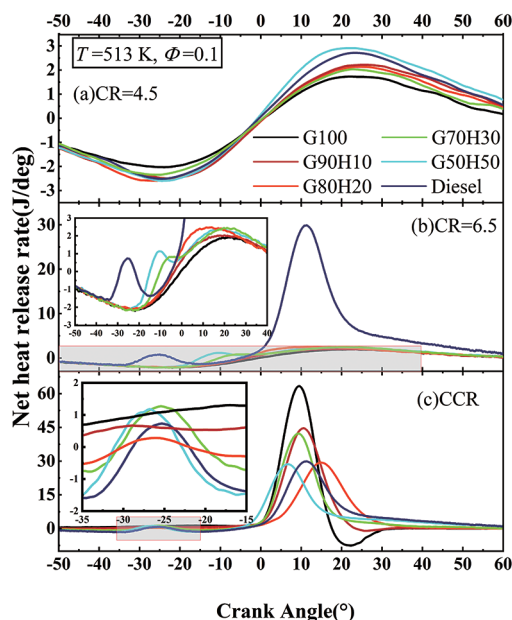
Figure 6. Effect of blending ratio on the net heat release rate of gasoline/HCB blends under different compression ratios: (**a**) CR = 4.5, (**b**) CR = 6.5, (**c**) CCR.

In Figure 6b, as the compression ratio increases to 6.5, distinct differences in the heat release rates among different fuels begin to emerge. Diesel exhibits a pronounced two-stage heat release characteristic, namely, the phenomenon of compression ignition. Meanwhile, it is seen that other fuels continue to

undergo low-temperature oxidation heat release, whereby the peak low-temperature heat release progressively rises with increasing blend ratio. Furthermore, with the increase in blending ratio, the low-temperature heat release phase advances, and the low-temperature heat release trend becomes increasingly prominent.

Figure 6c illustrates the heat release rate of the fuels at their corresponding CCRs. The low-temperature heat release characteristics of the blended fuels can be observed from the pre-ignition. Low-temperature heat release occurs within a temperature range of approximately $-35°C$ to $-15°C$. Among them, G100 and G90H10 exhibit a single-peak heat release without distinct secondary heat release characteristics. From G80H20 onwards, a notable secondary heat release phenomenon becomes apparent. Moreover, the secondary heat release phenomena are seen to be more prominent in G70H30, G50H50, and diesel fuels. When the blending ratio is less than 20%, the low-temperature oxidation activity is weaker, and the phase of the main peak heat release will be delayed as the blending ratio increases. However, when the blending ratio exceeds 20%, the low-temperature oxidation activity strengthens, resulting in the occurrence of noticeable secondary heat release. In this case, the phase of the main peak heat release advances as the blending ratio increases.

3.2. Effect of Equivalence Ratio on the Low-Temperature Oxidation Characteristics of Blended Fuels

The equivalence ratio has a significant impact on the low-temperature oxidation characteristics and compression ignition of the fuel. Both the excessively low and high equivalence ratios can influence the low-temperature oxidation characteristics, thereby affecting the stability and quality of compression ignition. Hence, investigating the influence of different intake temperatures on the low-temperature oxidation characteristics of blended fuels is highly necessary.

Figure 7 illustrates the CO emissions and maximum in-cylinder temperature variations of the G80H20 as a function of compression ratio under different equivalence ratio conditions, with an intake temperature of 513 K. The bar chart depicts the corresponding magnitudes of their increase rates. From Figure 7a, it can be observed that the peak CO emissions are approximately 6000, 8000, and 9000 ppm corresponding to the equivalence ratios of 0.1, 0.15, and 0.2, respectively. With the increase of equivalence ratio, the peak of CO emissions increases significantly, but the rate of increase gradually slows down. At the same compression ratio, the higher equivalence ratios result in higher CO emissions. This phenomenon occurs due to the fuel undergoing a low-temperature reaction before reaching the CCR and subsequent ignition. During this pathway, the active radicals and energy gradually accumulate, ultimately triggering ignition. During low-temperature reactions, the accumulation of radicals primarily originates from the addition of dual oxygen fuel molecule radicals and subsequent chain branching and chain propagation reactions [35,36]. An increase in the equivalence ratio promotes the progression of the low-temperature reaction pathway in the forward direction, thereby enhancing the low-temperature oxidation activity and increasing CO emissions. It can be observed from Figure 7b that, with an increasing equivalence ratio of every 0.05 value within the LTO region, the CO rise magnitude increases by approximately 2000. Simultaneously, within the NTC region, the CO rise magnitude also exhibits a similar trend, increasing by approximately 1000 with an increasing equivalence ratio of every 0.05 value.

It can be observed from Figure 7c that during the low-temperature oxidation phase, the maximum in-cylinder temperature increases linearly with the increase of compression ratio. At the same compression ratio, the maximum in-cylinder temperature of G80H20 increases with the rise in equivalence ratio. During the high-temperature combustion phase, the increased equivalence ratio results in elevated fuel energy, consequently leading to an increase in the maximum in-cylinder temperature. In Figure 7d, the magnitude of the increase in maximum in-cylinder temperature shows a consistent upward trend as the equivalence ratio increases.
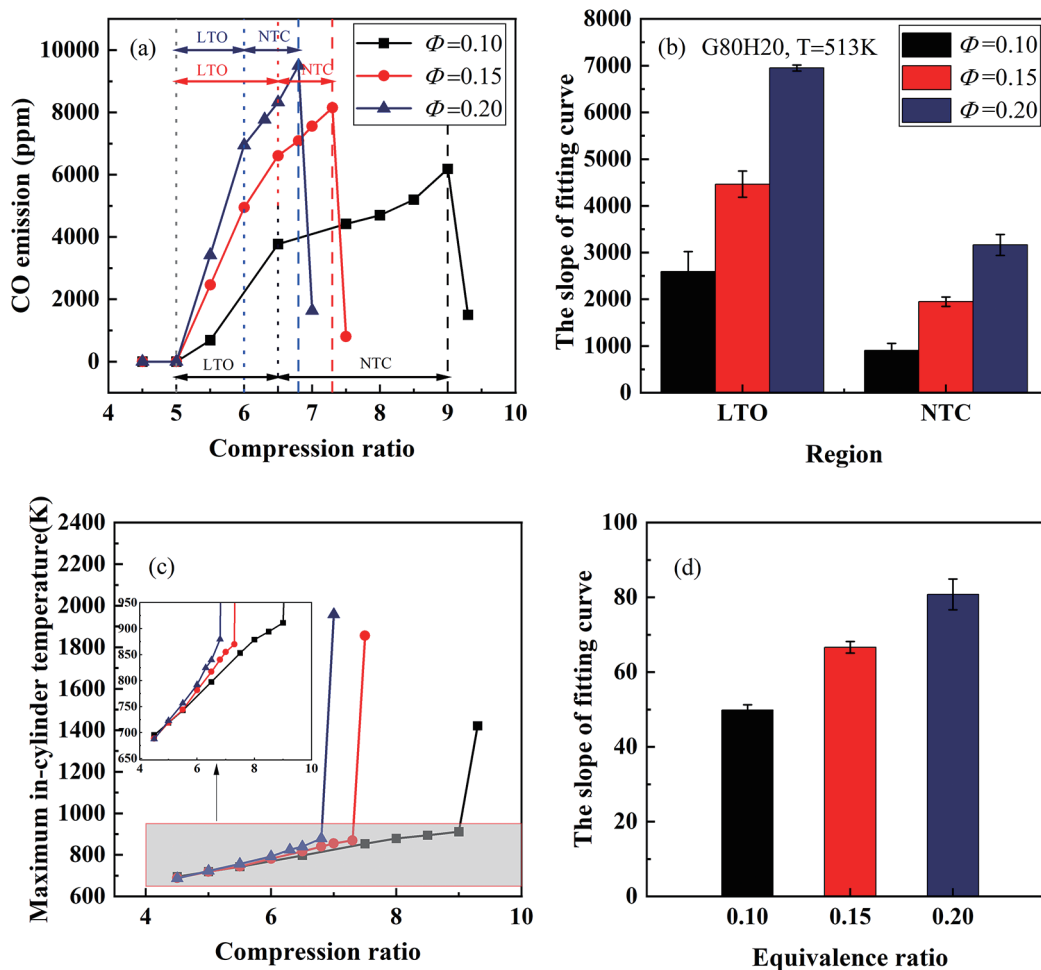
Figure 7. (**a**) CO Emissions, (**b**) CO Emissions Fit Curve Slope, (**c**) Maximum In-Cylinder Temperature, (**d**) Maximum In-Cylinder Temperature Fit Curve Slope for G80H20 at different equivalence ratio.

Figure 8 depicts the ignition boundaries of G80H20 to different equivalence ratios at an intake temperature of 513 K. From Figure 8a, it can be observed that as the equivalence ratio gradually increases from 0.10 to 0.15 and 0.20, CCR of G80H20 is 9.3, 7.5, and 7.0, respectively. It is noted that the variation magnitude of critical compression ratios is greater in the range of equivalence ratios from 0.10 to 0.15 than in the range of 0.15 to 0.20. The findings suggest that as the equivalence ratio increases, the sensitivity of the CCR of the blended fuel to the equivalence ratio decreases. From Figure 8b, it can be observed that as the equivalence ratio increases, critical temperatures of G80H20 exhibit the following characteristics. Specifically, as the equivalence ratio is raised to 0.15, a notable reduction in critical temperature is observed. Subsequently, when the equivalence ratio is further increased from 0.15 to 0.20, a small rise in critical temperature is observed. In conclusion, the increase in equivalence ratio from 0.1 to 0.15 has a more significant impact on the ignition boundaries compared to the increase from 0.15 to 0.2.
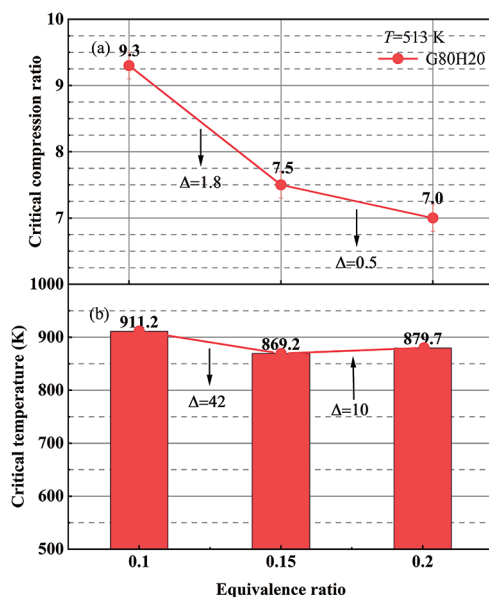
Figure 8. (**a**) Critical Compression Ratio and (**b**) Critical Temperature of G80H20 for different equivalence ratios.

Figure 9 shows the heat release rate of G80H20 at three different compression ratios of 4.5, 6.5, and CCR. From Figure 9a, it is evident that the increasing equivalence ratio has no effect on the heat release rate, confirming that no low-temperature oxidation reaction occurs in the fuel at CR = 4.5. This confirms the NO-load curve where there is no low-temperature oxidation phenomenon in the fuel. Figure 9c illustrates the heat release rate curve at CCR. It can be observed that the main peak heat release experiences a significant increase between 0.1 and 0.15, while the increase from 0.15 to 0.2 is very small. A zoomed-in view highlights the low-temperature heat release phenomenon with a consistent onset time, but with higher heat release at lower equivalence ratios.
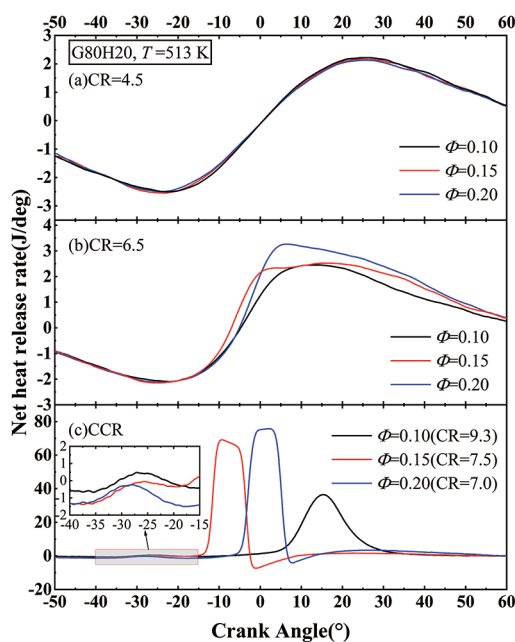

Figure 9. Effect of equivalence ratio on the in-cylinder net heat release rate of G80H20 under different compression ratios: (**a**) CR = 4.5, (**b**) CR = 6.5, (**c**) CCR.

3.3. Effect of Intake Temperature on the Low-Temperature Oxidation Characteristics of Blended Fuels

The low-temperature oxidation characteristics of fuel are highly sensitive to the initial temperature [37,38]. Therefore, it is necessary to determine the appropriate intake temperature to investigate the impact of different intake temperatures on the low-temperature oxidation characteristics of the blended fuel.

Figure 10 illustrates the variations of CO emissions, as well as the peak in-cylinder temperature of the G50H50, with different compression ratios at three intake temperatures (433 K, 473 K, and 513 K). Additionally, the corresponding bar charts depict the changes in their respective increments. In Figure 10a, it can be observed that during the low-temperature oxidation phase, there is little variation in the peak CO emission levels among the fuels. When the intake temperature is increased from 433K to 473K, the peak slightly decreases; however, when the intake temperature is increased to 513K, the peak remains unchanged. Furthermore, at the same compression ratio, higher intake temperatures are associated with higher CO emission levels. In contrast, in Figure 10b, it is evident that the magnitude of CO emission increase is not simply proportional to the rise in intake temperature. Within the LTO region, the increment first rises and then diminishes as the intake temperature increases. Conversely, in the NTC region, the extent of CO decreases with higher intake temperatures.
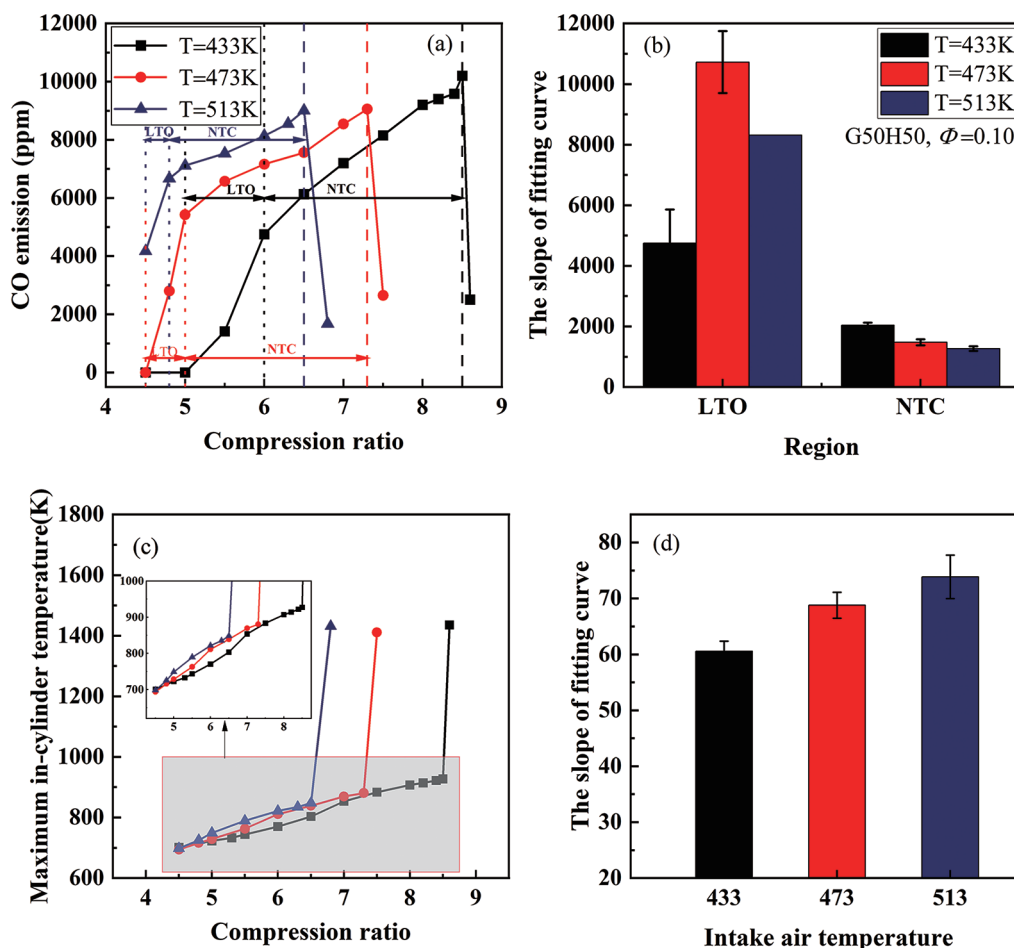

Figure 10. (**a**) CO Emissions, (**b**) CO Emissions Fit Curve Slope, (**c**) Maximum In-Cylinder Temperature, (**d**) Maximum In-Cylinder Temperature Fit Curve Slope for G50H50 at different intake temperature.

Figure 10c shows that the increasing compression ratio shows a gradual linear rise in the peak in-cylinder temperature. Moreover, under the same compression ratio, higher intake temperatures lead to higher maximum in-cylinder temperatures. It can also be observed that the maximum in-cylinder temperature during ignition is hardly influenced by the intake temperature because of the same equivalence ratio. In Figure 10d, it can be observed that the increasing intake temperature tends to a gradual rise in the magnitude of the

increase in the maximum in-cylinder temperature during the low-temperature oxidation phase.

Figure 11 depicts the variations in the ignition boundary characteristics of the G50H50 at different intake temperatures. From Figure 11a the change in CCR of G50H50 with respect to the intake temperature shows that, as the intake temperature increases from 433 K to 513 K the CCR of G50H50 decreases from 8.6 to 6.8 and this decreasing trend remains relatively consistent. From Figure 11b the increasing intake temperature decreases the critical temperature of G50H50 at a uniform rate. Similar to CCR, the change in the rate of ignition boundary decrease is quite small as the intake temperature rises.
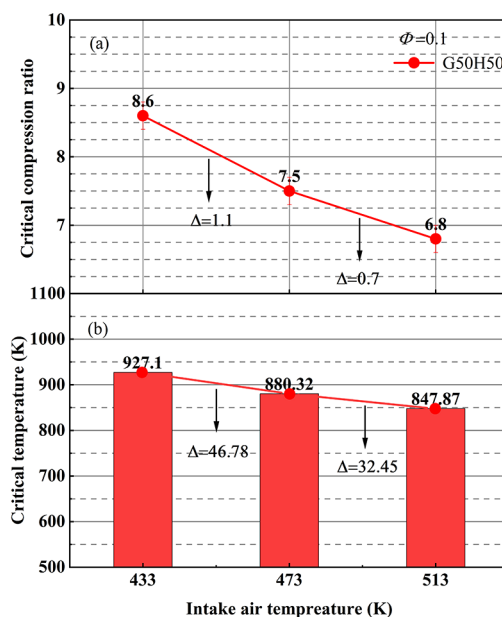

Figure 11. (**a**) Critical Compression Ratio and (**b**) Critical Temperature of G50H50 at different intake temperatures.

Figure 12 displays the heat release rate of G50H50 at three intake temperatures (433 K, 473 K, and 513 K) and three compression ratios (5.0, 6.0, and CCR). Based on the observation from Figure 12a, we can note that at T = 433 K and CR = 5.0, no CO emissions are generated as indicated by Figure 10 implying the absence of low-temperature oxidation phenomena. The heat release rate curve at this point corresponds to the NO-load condition. With the increase in intake temperature, the phenomenon of low-temperature heat release emerges, and the heat release phase advances.

From Figure 12b, as the compression ratio increases to 6.0, the phenomenon of low-temperature heat release becomes more pronounced. At an intake temperature of 433 K, the net heat release rate increases, and the phenomenon of low-temperature heat release begins to emerge. While at the two remaining intake temperatures, the low-temperature heat release phase advances by 10 degrees. As the compression ratio is increased there is a corresponding increase in in-cylinder pressure and temperature. Consequently, this rise facilitates the low-temperature oxidation process, leading to the advanced heat release phase.

From Figure 12c, considering the CCR condition, it is evident that the low-temperature peak heat release of the fuel decreases and advances as the intake temperature increases. The reason for this phenomenon can be attributed to the fact that increasing intake temperature results in higher in-cylinder temperatures during the initial stage of compression. Consequently, this leads to an earlier initiation of the low-temperature oxidation phase. The reduction in low-temperature oxidation activity at the ignition timing leads to a decrease in the peak for low-temperature heat release, which can be attributed to the relatively lower temperatures. By comparing the main peak heat release of the fuel at temperatures of 433 K and 473 K, the main heat release peak of the fuel develops earlier at 433 K. This can be attributed to the higher pressure and temperature at the end of compression. Even though the temperature at the end of compression is lower at 513 K than at 473 K, the early release of low-temperature heat has a bigger effect on fuel reactivity. As a result, the main peak heat release appears earlier than before.
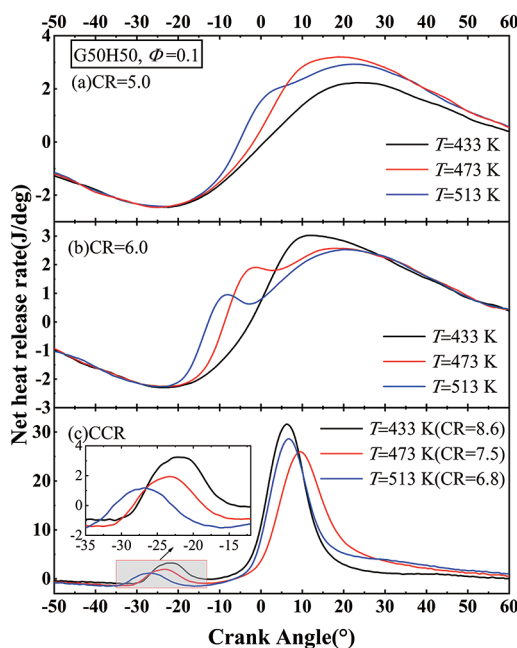
Figure 12. Effect of intake temperatures on in-cylinder net heat release rate of G50H50 under different compression ratios: (**a**) CR = 5.0, (**b**) CR = 6.0, (**c**) CCR.

4. Conclusions

This study investigates the ignition characteristics of the gasoline-HCB blends, as well as pure gasoline and diesel fuels during different compression ratios. In the study, the effects of equivalence ratio and intake temperature on the behavior of the blended fuel are taken into account. An investigation was carried out to analyze the low-temperature oxidation characteristics, ignition boundaries, and heat release rates of various fuels at different compression ratios. The study aimed to understand the influence of blending ratios, equivalence ratios, and intake temperatures on the behavior of the blended fuel. The key conclusions of this study are as follows:

(1) Increasing the blending ratio enhanced the low-temperature oxidation characteristics of the blended fuel. Simultaneously, the ignition boundaries decrease rapidly, but the rate of decrease subsequently slows down. A significant rise in carbon monoxide (CO) emissions is observed in the low-temperature combustion (LTC) area when the blending ratio exceeds 20%. The rate is minimally affected by further raising the blending ratio. Moreover, a distinct secondary heat release event is observed during the ignition process, which also impacts the heat release phase of the primary peak heat release.

(2) When comparing G50H50 to diesel, it is seen that they exhibit comparable low-temperature oxidation characteristics and compression ignition behavior when subjected to near-ignition boundary conditions. Hence, it may be suggested that G50H50 exhibits considerable promise as a viable substitute for diesel fuel in compression engines.

(3) The increase in equivalency ratio from 0.1 to 0.15 has a more pronounced effect on improving low-temperature oxidation characteristics, reducing ignition boundaries, and increasing the maximum heat release rate during ignition compared to the increase from 0.15 to 0.2.

(4) The enhancement of low-temperature oxidation characteristics is observed with the rise in intake temperature. Especially at 473K, the CO emission in the LTC zone exhibits the most significant rise, whereas the rate of increase in the NTC region gradually reduces. Moreover, the ignition boundaries also showed a consistent linear decline. Simultaneously, the peak low-temperature heat release diminishes, and the heat release phase advances during ignition.

Author Contributions: Conceptualization, S.L. and, W.Z.; methodology, W.Z.; formal analysis, S.L.; resources, Q.W.; data curation, W.Z.; writing—original draft preparation, S.L.; writing—review and editing, T.P.; supervision, W.Z.;

References

1. Possession of Civil Vehicle. National Bureau of Statistics of China. Available online: https://www. stats. gov. cn/ (Accessed on 25 September 2023).
2. Jia, M.; Xie, M. A chemical kinetics model of iso-octane oxidation for HCCI engines. *Fuel* **2006**, *85*(17–18), 2593–2604.
3. Niklawy, W.; Shahin, M.; Amin, M. I.; et al. Comprehensive analysis of combustion phasing of multi-injection HCCI diesel engine at different speeds and loads. *Fuel* **2022**, *314*, 123083.
4. Kiplimo, R.; Tomita, E.; Kawahara, N.; et al. Effects of spray impingement, injection parameters, and EGR on the combustion and emission characteristics of a PCCI diesel engine. *Applied Thermal Engineering* **2012**, *37*, 165–175.
5. Agarwal, A.K.; Singh, A.P.; Kumar, V. Particulate characteristics of low-temperature combustion (PCCI and RCCI) strategies in single cylinder research engine for developing sustainable and cleaner transportation solution. *Environmental Pollution* **2021**, *284*, 117375.
6. Okcu, M.; Varol, Y.; Altun Ş.; et al. Effects of isopropanol-butanol-ethanol (IBE) on combustion characteristics of a RCCI engine fueled by biodiesel fuel. *Sustainable Energy Technologies and Assessments* **2021**, *47*, 101443.
7. Khaled, F.; Javed, T.; Farooq, A.; et al. Analysis of ignition temperature range and surrogate fuel requirements for GCI engine. *Fuel* **2022**, *312*, 122978.
8. Putrasari, Y.; Lim, O. A study on combustion and emission of GCI engines fueled with gasoline-biodiesel blends. *Fuel* **2017**, *189*, 141–154.
9. Johansson, B. High-load partially premixed combustion in a heavy-duty diesel engine. In *Diesel engine emissions reduction (DEER) Conference. Chicago, Illinois*, USA. 2005 *(*pp. 21–25). Available online: https://www.mscc.se/wp-content/uploads/2011/11/HCCI-och-PPC-2005_deer_johansson.pdf (Accessed on 25 September 2023).
10. Hildingsson, L.; Johansson, B.; Kalghatgi, G. T.; et al. Some effects of fuel autoignition quality and volatility in premixed compression ignition engines. *SAE International Journal of Engines* **2010**, *3*(1), 440–460.
11. Ra, Y.; Loeper, P.; Reitz, R.; et al. Study of high speed gasoline direct injection compression ignition (GDICI) engine operation in the LTC regime. *SAE International Journal of Engines* **2011**, *4*(1), 1412–1430.
12. Hanson, R.; Splitter, D.; Reitz, R. D. Operating a heavy-duty direct-injection compression-ignition engine with gasoline for low emissions. *SAE Technical Paper* **2009**, No. 2009-01-1442.
13. Weall, A.; Collings, N. Investigation into partially premixed combustion in a light-duty multi-cylinder diesel engine fuelled with a mixture of gasoline and diesel. *SAE Technical Paper* **2007**, No. 2007-01-4058.
14. Kolodziej, C.; Kodavasal, J.; Ciatti, S.; et al. Achieving stable engine operation of gasoline compression ignition using 87 AKI gasoline down to idle. *SAE Technical Paper* **2015**, No. 2015-01-0832.
15. Yang, H.; Shuai, S.; Wang, Z.; et al. Fuel octane effects on gasoline multiple premixed compression ignition (MPCI) mode. *Fuel* **2013**, *103*, 373–379.
16. Kodavasal, J.; Kolodziej, C.; Ciatti, S.; et al. CFD simulation of gasoline compression ignition. In *Internal Combustion Engine Division Fall Technical Conference.* American Society of Mechanical Engineers. 2014. Vol. 46179, p. V002T06A008
17. Manente, V.; Zander, C.G.; Johansson, B.; et al. An advanced internal combustion engine concept for low emissions and high efficiency from idle to max load using gasoline partially premixed combustion. *SAE Technical Paper* **2010**, No. 2010-01-2198.
18. Zhang, F.; Xu, H.; Rezaei, S. Z.; et al. Combustion and emission characteristics of a PPCI engine fuelled with dieseline. *SAE Technical Paper* **2012**, No. 2012-01-1138.
19. Zhang, F.; Xu, H.; Zhang, J.; et al. Investigation into light duty dieseline fuelled partially-premixed compression ignition engine. *SAE International Journal of Engines* **2011**, *4*(1), 2124–2134.
20. Adams, C. A.; Loeper, P.; Krieger, R.; et al. Effects of biodiesel – gasoline blends on gasoline direct-injection compression ignition (GCI) combustion. *Fuel* **2013**, *111*, 784–790.
21. Zhong, W.; Yuan, Q.; Liao, J.; et al. Experimental and modeling study of the autoignition characteristics of gasoline/ hydrogenated catalytic biodiesel blends over low-to-intermediate temperature. *Fuel* **2022**, *313*, 122919.
22. Wang, Z.; Liu, H.; Reitz, R.D. Knocking combustion in spark-ignition engines. *Progress in Energy and Combustion Science* **2017**, *61*, 78–112.
23. Han, W.Q.; Yao, C.D. Research on high cetane and high octane number fuels and the mechanism for their common oxidation and auto-ignition. *Fuel* **2015**, *150*, 29–40.
24. Kang, D.; Kim, D.; Kalaskar, V.; et al. Experimental characterization of jet fuels under engine relevant conditions– Part 1: Effect of chemical composition on autoignition of conventional and alternative jet fuels. *Fuel* **2019**, *239*, 1388–1404.
25. Wu, S.; Kang, D.; Zhang, H.; et al. The oxidation characteristics of furan derivatives and binary TPGME blends

under engine relevant conditions. *Proceedings of the Combustion Institute* **2019**, *37*(4), 4635–4643.

26. Kang, D.; Kalaskar, V.; Kim, D.; et al. Experimental study of autoignition characteristics of Jet-A surrogates and their validation in a motored engine and a constant-volume combustion chamber. *Fuel* **2016**, *184*, 565–580.

27. Kang, D.; Bohac, S.V.; Boehman, A.L.; et al. Autoignition studies of C5 isomers in a motored engine. *Proceedings of the Combustion Institute* **2017**, *36*(3), 3597–3604.

28. Glassman, I.; Yetter, R.A. *Combustion*. 4th ed.; Academic Press: Boston, MA, USA, 2008.

29. Natelson, R. H.; Kurman, M. S.; Cernansky, N. P.; et al. Low temperature oxidation of n-butylcyclohexane. *Combustion and Flame* **2011**, *158*(12), 2325–2337.

30. Zhou, Y.; Gan, Y.; Gou, X. Chemical kinetic modeling study of methyl esters oxidation: Improvement on the prediction of early CO2 formation. *Fuel* **2020**, *279*, 118383.

31. Kang, D.; Bohac, S.V.; Boehman, A.L.; et al. Autoignition studies of C5 isomers in a motored engine. *Proceedings of the Combustion Institute* **2017**, *36*(3), 3597–3604.

32. Wang, Z.; Popolan-Vaida, D. M.; Chen, B.; et al. Unraveling the structure and chemical mechanisms of highly oxygenated intermediates in oxidation of organic compounds. *Proceedings of the National Academy of Sciences* **2017**, *114*(50), 13102–13107.

33. Curran, H.J.; Gaffuri, P.; Pitz, W.J.; et al. A comprehensive modeling study of n-heptane oxidation. *Combustion and Flame* **1998**, *114*(1–2), 149–177.

34. Curran, H.J.; Gaffuri, P.; Pitz, W.J.; et al. A comprehensive modeling study of iso-octane oxidation. *Combustion and Flame* **2002**, *129*(3), 253–280.

35. Cox, R. A.; Cole, J. A. Chemical aspects of the autoignition of hydrocarbon air mixtures. *Combustion and Flame* **1985**, *60*(2), 109–123.

36. Curran, H.J. Developing detailed chemical kinetic mechanisms for fuel combustion. *Proceedings of the Combustion Institute* **2019**, *37*(1), 57–81.

37. Khaled, F.; Javed, T.; Farooq, A.; et al. Analysis of ignition temperature range and surrogate fuel requirements for GCI engine. *Fuel* **2022**, *312*, 122978.

38. Zhu, J.; Wang, S.; Raza, M.; et al. Autoignition behavior of methanol/diesel mixtures: Experiments and kinetic modeling. *Combustion and Flame* **2021**, *228*, 1–12.

Publisher's Note: Scilight stays neutral with regard to jurisdictional claims in published maps and institutional affiliations.